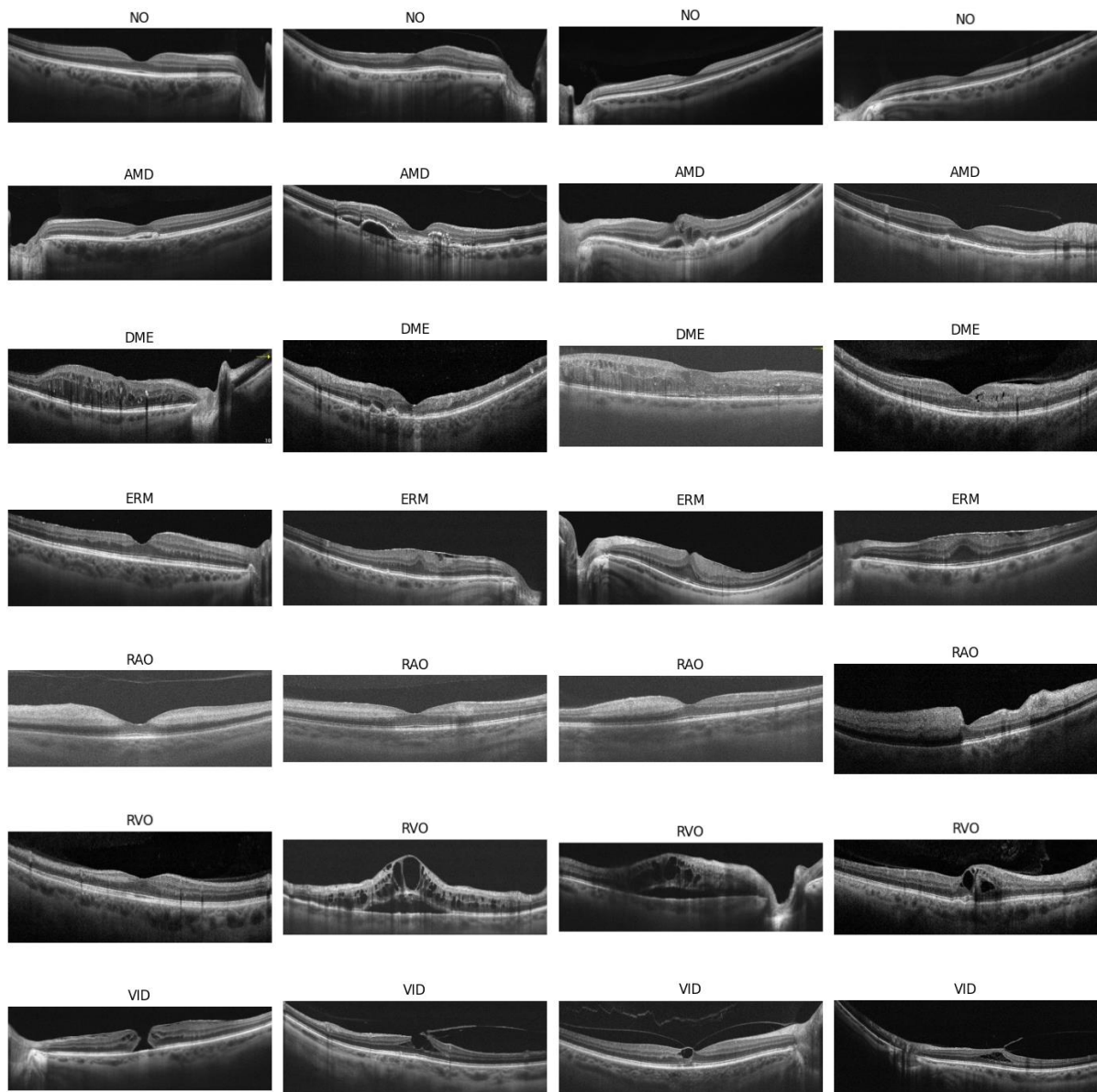


Ocular Disorders Detection with Deep Learning Approach Using Optical Coherence Tomography (OCT) Images



Background

Optical Coherence Tomography (OCT) and fundus photography are pivotal non-invasive imaging techniques utilized for the detection and monitoring of various ocular conditions. OCT employs light waves to capture high-resolution cross-sectional images of the retina, enabling detailed examination of its layers¹. The application of OCT in diagnosing ocular disorders such as glaucoma², diabetic retinopathy³, and age-related macular degeneration (AMD)⁴ has been extensively documented, highlighting its significance in clinical ophthalmology.

Both OCT and fundus images have been instrumental in training deep neural networks for developing computer-aided diagnostic systems. Numerous datasets, including both open-access and limited-access collections, exist for these imaging modalities^{5,6}. The Kermany dataset⁷ is recognized as one of the most comprehensive collections of OCT images available.

Additionally, Yoo et al. (2020) previously shared an open-access dataset that is now the second largest publicly available collection of OCT images, comprising 2,064 images across seven ocular conditions, including normal retinal images. However, this dataset presents a significant class imbalance; AMD constitutes the majority with 1,231 images, while retinal artery occlusion (RAO) is represented by only 22 images.

While deep learning models can exhibit robustness against class imbalances, they are not entirely immune to its effects. Consequently, specific techniques may be necessary to enhance model performance in such scenarios. The objective of this project is to fine-tune a pre-trained model, EfficientNet, while exploring the efficacy of adjusting class weights to address class imbalance issues.

Dataset

The OCTDL dataset utilized in this project is accessible via Mendeley and comprises a total of 2,064 OCT images stored in JPG format. These images are organized into separate folders corresponding to specific disease labels. The dataset includes macular raster scans for several ocular conditions, including Age-related Macular Degeneration (AMD), Diabetic Macular Edema (DME), Epiretinal Membrane (ERM), Retinal Artery Occlusion (RAO), Retinal Vein Occlusion (RVO), and Vitreomacular Interface Disease (VID). Additionally, it features various pathological conditions such as Macular Neovascular Membranes (MNV), Disorganization of Retinal Inner Layers (DRIL), drusen, Macular Edema (ME), and Macular Hole (MH).

For model development, data splitting was performed following the methodology outlined by Kulyabin et al. (2024). The dataset was randomly divided into training, validation, and test subsets in a ratio of 70:10:20 at the patient level. This approach ensures that images from a single patient are exclusively allocated to one of the subsets, thereby preventing data leakage and promoting the robustness of the model evaluation. Used data is available at the following link and can be accessed for free: <https://data.mendeley.com/datasets/btv6yrdbmv/1>

Table 1. Class distribution of OCTDL dataset.

Disorder	Label	Number of OCT Images	Number of Patients
Age-related Macular Degeneration	AMD	1231	421
Diabetic Macular Edema	DME	147	107
Epiretinal Membrane	ERM	155	71
Normal	NO	332	110
Retinal Artery Occlusion	RAO	22	11
Retinal Vein Occlusion	RVO	101	50
Vitreomacular Interface Disease	VID	76	51
Total		2064	821

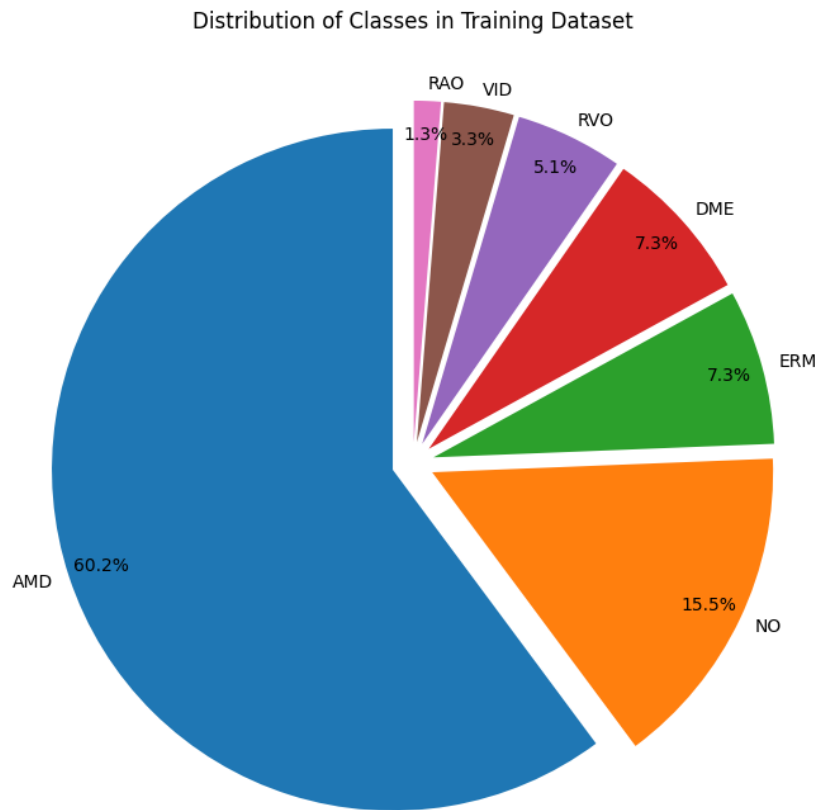


Figure 1. Proportion of each ocular conditions in the dataset.

Data Preprocessing

All images were rescaled to a pixel intensity range of 0 to 1 to normalize the input data. To enhance the diversity of the training dataset and prevent overfitting, data augmentation techniques were applied. The augmentation strategies included random rotations up to 0.2 radians, width and height shifts of up to 10%, zoom adjustments within a 0.2 range, as well as horizontal and vertical flips. These techniques were implemented to improve the model's ability to generalize across variations in the input data.

Results

Yoo et al. (2020) previously trained their models using two pre-trained architectures, VGG16 and ResNet50, on the OCTDL dataset. Given the significant class imbalance in this dataset, this project aimed to leverage class weight adjustment while fine-tuning models with a different architecture. Specifically, two models were fine-tuned using the EfficientNetV2 architecture. Both models were based on the EfficientNetV2 framework, with one model incorporating class weight adjustments during training. In this approach, higher weights were assigned to the minority classes to mitigate the effects of class imbalance. For clarity, the model without class weight adjustment is referred to as Model 1, while the model with class weight adjustment is referred to as Model 2.

Model 1 and Model 2 achieved accuracies of 90.91% and 90.42%, respectively, on the test dataset. The primary objective of this project was to investigate whether adjusting class weights could improve model performance in an imbalanced OCT image classification task. Based on the results presented in Table 2, while the application of class weights (Model 2) led to marginal improvements in specific classes, such as Diabetic Macular Edema (DME), it did not result in a consistent overall performance boost. In fact, Model 2 underperformed compared to Model 1 (without class weights) in metrics for most classes, particularly in detecting rare conditions like Retinal Artery Occlusion (RAO) and Vitreomacular Interface Disease (VID). Additionally, Model 2 exhibited decreased Precision and F1-Score in several instances.

These findings suggest that while class weight adjustment may help address class imbalance to some extent, it can also introduce trade-offs that negatively affect overall model performance. This highlights the need for more sophisticated strategies to effectively handle imbalanced datasets.

Table 2. Resulting metrics of Model 1 (without class weight adjustment) and Model 2 (with class weight adjustment) on OCTDL dataset.

Class	Model	Precision	Recall	F1-Score	AUC	Average Precision
AMD	Model 1	0.9705	0.9664	0.9684	0.9936	0.9960
	Model 2	0.9745	0.9622	0.9683	0.9898	0.9938
DME	Model 1	0.6452	0.6897	0.6667	0.9853	0.8406
	Model 2	0.7241	0.7241	0.7241	0.9768	0.8321
ERM	Model 1	0.8286	0.9667	0.8923	0.9933	0.9592
	Model 2	0.7778	0.9333	0.8485	0.9935	0.9706
NO	Model 1	0.8767	0.9412	0.9078	0.9940	0.9659
	Model 2	0.9231	0.8824	0.9023	0.9945	0.9704
RAO	Model 1	1.0000	1.0000	1.0000	1.0000	1.0000
	Model 2	0.7500	1.0000	0.8571	1.0000	1.0000
RVO	Model 1	0.7500	0.3913	0.5143	0.9711	0.7337
	Model 2	0.5789	0.4783	0.5238	0.9561	0.6928
VID	Model 1	0.9375	0.9375	0.9375	1.0000	1.0000
	Model 2	0.8421	1.0000	0.9143	0.9997	0.9931

Receiver Operating Characteristic (ROC) Curve

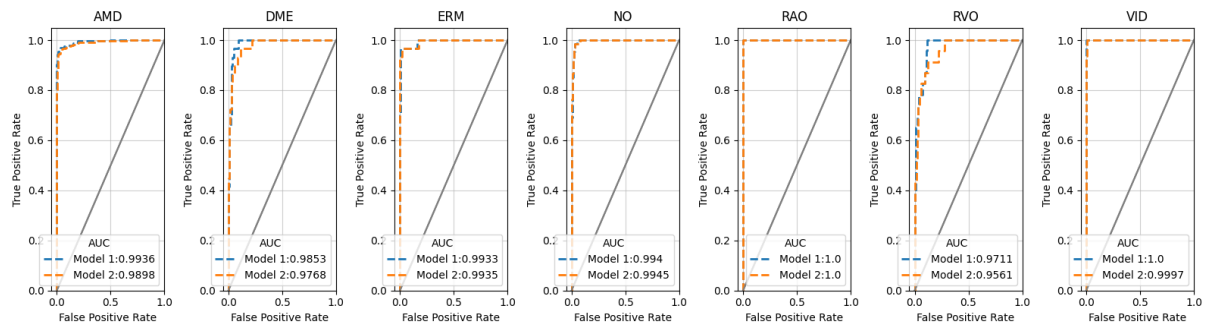


Figure 2. Receiver Operating Characteristic (ROC) curves.

Precision Recall Curve

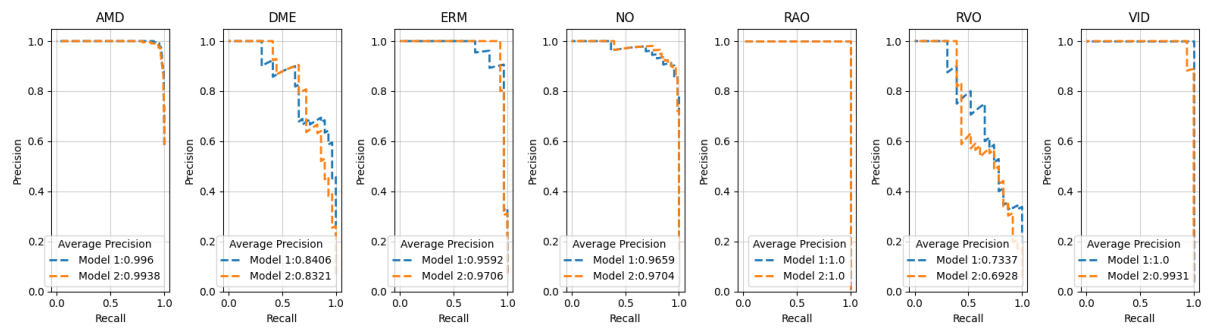


Figure 3. Precision recall curves.

Confusion Matrix

		Model 1									Model 2						
Actual	AMD	230	2	0	6	0	0	0	Actual	AMD	229	1	1	3	0	4	0
	DME	1	20	4	0	0	3	1		DME	2	21	0	0	0	3	3
	ERM	0	0	29	1	0	0	0		ERM	0	1	28	1	0	0	0
	NO	3	0	1	64	0	0	0		NO	2	1	4	60	0	1	0
	RAO	0	0	0	0	3	0	0		RAO	0	0	0	0	3	0	0
	RVO	3	8	1	2	0	9	0		RVO	2	5	3	1	1	11	0
	VID	0	1	0	0	0	0	15		VID	0	0	0	0	0	0	16
		AMD	DME	ERM	NO	RAO	RVO	VID			AMD	DME	ERM	NO	RAO	RVO	VID
		Predicted									Predicted						

Figure 4. Confusion matrices of models fine-tuned using EfficientNetv2 architecture, Model 1 (without class weight adjusted) and Model 2 (with class weight adjusted), trained on OCTDL dataset.

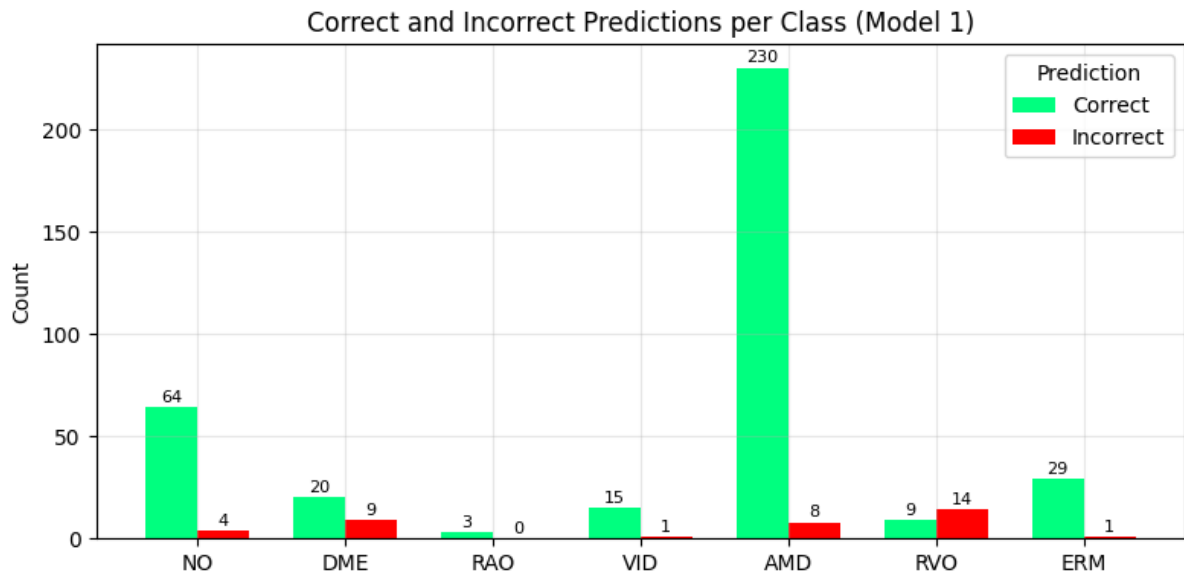


Figure 5. Correct and incorrect predictions for each class by Model 1.

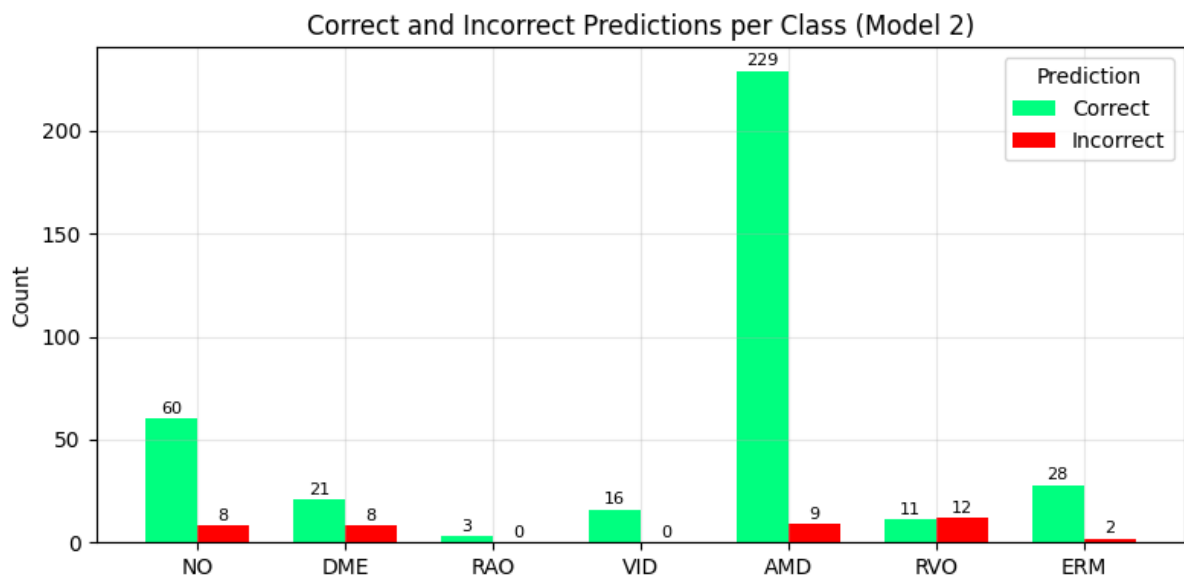


Figure 6. Correct and incorrect predictions for each class by Model 2.

Error Analysis

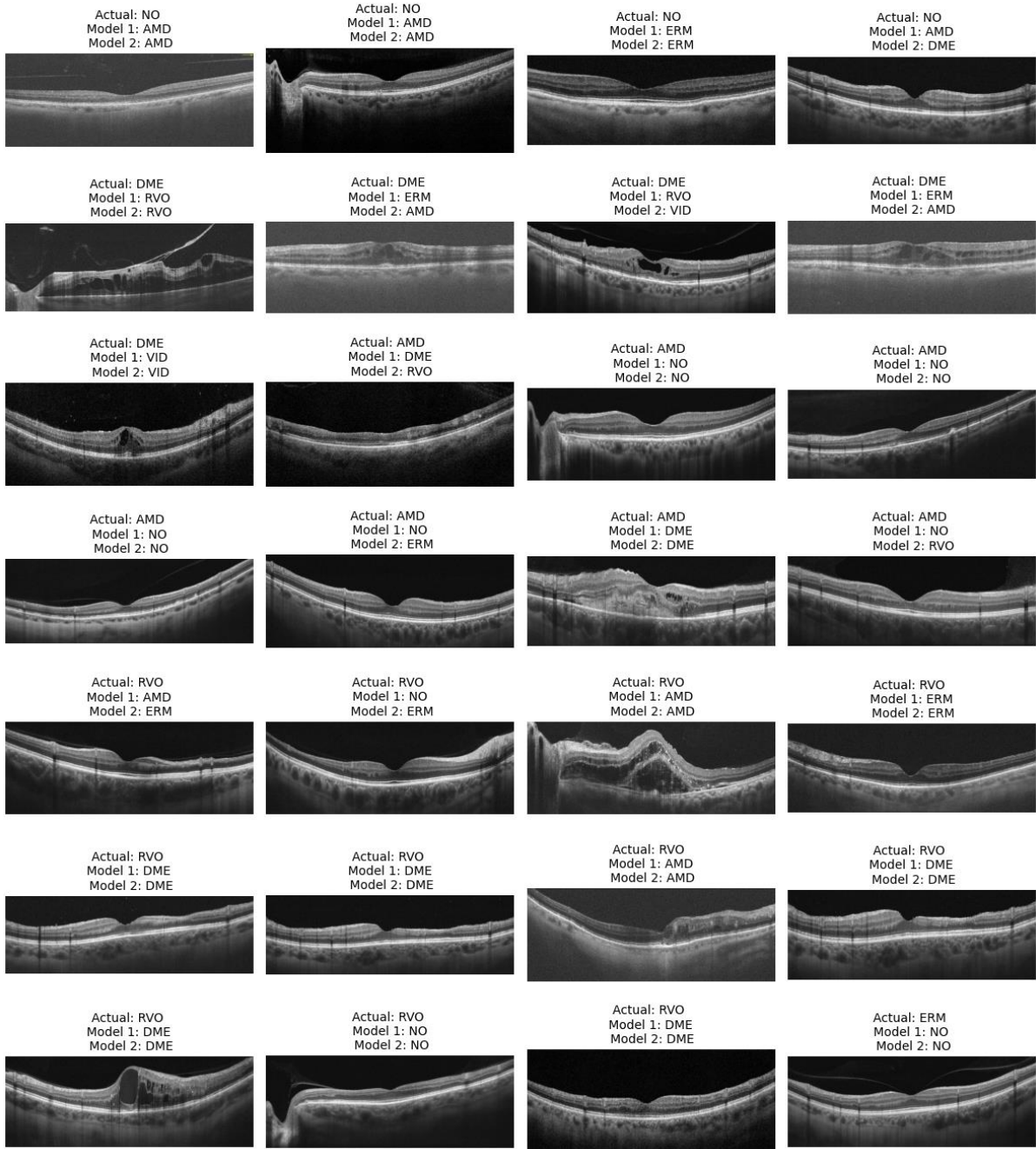


Figure 7. Images failed to classify by both models.

Future Directions

- **Addressing Class Imbalance.** Exploring additional techniques such as oversampling and undersampling be applied to enhance the model's ability to generalize and improve overall performance. These methods may help mitigate the effects of class imbalance in the dataset, leading to more robust predictions across all classes.
- **Exploring Vision Transformers.** Investigating the use of pre-trained Vision Transformer (ViT) models could be beneficial for assessing their performance, particularly concerning minority classes. Given their unique architecture and attention mechanisms, ViTs may offer improved feature extraction and classification capabilities compared to traditional CNNs.
- **Image Enhancement Techniques.** Recent work by Elkholy et al. (2024) indicates that image enhancement techniques—including brightness and contrast adjustments, as well as smoothing methods to reduce blur and noise—can significantly improve model performance. Their findings suggest that these enhancements achieved accuracy levels surpassing those reported in previous literature using the Kermany OCT dataset. Exploring similar image enhancement strategies may provide valuable insights for future research.
- **Combining Image Modalities.** Investigating the integration of multiple imaging modalities, such as OCT and fundus photography, in model training. This approach aims to leverage the complementary strengths of each modality, enhancing feature extraction and providing a more comprehensive understanding of ocular conditions. Models trained with diverse data modalities are likely to exhibit greater diagnostic robustness, effectively mitigating variability associated with individual imaging techniques.

Reference

1. Optical Coherence Tomography (OCT) and Fundus Photography. <https://www.oscarwylee.com.au/glasses/eye/oct-fundus-test?srsId=AfmBOoqtsC5Dn1sNvNc88jzjnj21SL3oKIPKYHzEMbCqiddTlfRNFmLx>
2. Geevarghese, A., Wollstein, G., Ishikawa, H., & Schuman, J. S. (2021). Optical Coherence Tomography and Glaucoma. *Annual review of vision science*, 7, 693–726.
3. Amoaku, W. M., Ghanchi, F., Bailey, C., Banerjee, S., Banerjee, S., Downey, L., Gale, R., Hamilton, R., Khunti, K., Posner, E., Quhill, F., Robinson, S., Setty, R., Sim, D., Varma, D., & Mehta, H. (2020). Diabetic retinopathy and diabetic macular oedema pathways and management: UK Consensus Working Group. *Eye (London, England)*, 34(Suppl 1), 1–51.
4. Flores, R., Carneiro, Â., Tenreiro, S., & Seabra, M. C. (2021). Retinal Progression Biomarkers of Early and Intermediate Age-Related Macular Degeneration. *Life (Basel, Switzerland)*, 12(1), 36.
5. Kulyabin, M., Zhdanov, A., Nikiforova, A., Stepichev, A., Kuznetsova, A., Ronkin, M., Borisov, V., Bogachev, A., Korotkich, S., Constable, P. A., & Maier, A. (2024). OCTDL: Optical Coherence Tomography Dataset for Image-Based Deep Learning Methods. *Scientific data*, 11(1), 365.
6. Krzywicki, T., Brona, P., Zbrzezny, A. M., & Grzybowski, A. E. (2023). A Global Review of Publicly Available Datasets Containing Fundus Images: Characteristics, Barriers to Access, Usability, and Generalizability. *Journal of clinical medicine*, 12(10), 3587.
7. Kermany, Daniel; Zhang, Kang; Goldbaum, Michael (2018), “Labeled Optical Coherence Tomography (OCT) and Chest X-Ray Images for Classification”, Mendeley Data, V2.

8. Yoo, TaeKeun (2020), "Data for: Improved accuracy in OCT diagnosis of rare retinal disease using few-shot learning with generative adversarial networks", Mendeley Data, V1.
9. Elkholy, M., & Marzouk, M. A. (2024). Deep learning-based classification of eye diseases using Convolutional Neural Network for OCT images. *Frontiers in Computer Science*, 5, 12522

